Fast Terahertz 3D Super-Resolution Surface Reconstruction by Variational Model from Limited Low-Resolution Sampling

Yiyao Zhang[12], Ke Chen[1] ,and Shang-Hua Yang[2]
[1]Centre for Mathematical Imaging Techniques, Department of Mathematical Sciences, University of Liverpool, Liverpool, L69 7ZL United Kingdom
[2]Institute of Electronics Engineering, Department of Electrical Engineering, National Tsing Hua University, Hsinchu, 30013 Taiwan

***Abstract*—Integrating with the signal processing, inverse Radon transform, and the variational model, the framework at least saving 83% data acquisition time for fast, smooth three-dimensional (3D) reconstruction from the limited dataset is elucidated in the field of terahertz imaging applications. In hot pursuit, under the viewpoint of discrete geometry, the quantifiable comparison for 3D surfaces by computing the standard deviation of mean curvatures is also proposed to show the reconstructed effectiveness from less input with gaps.**

I. Introduction

TERAHERTZ (THz) waves provide distinctive properties (e.g. spectral fingerprints, non-contact, and non-ionizing) with feasible applications in chemical identification, security screening as well as medical imaging. Based on its advantage, THz imaging has been recognized the necessity with the tool by THz time-domain spectroscopy (THz-TDS) system for visualizing object interior geometry and its material composition. In THz-TDS, its unique capability is to keep track of the rich features with the interaction between THz radiation and objects by the amplitude and the phase of the THz temporal/spectral signals [1]. Regrettably, the data acquisition by the THz-TDS system is highly time-consuming in accordance with the raster-scanning. Also, regarding the resolution of imaging applications associated with the THz wavelengths from around 100 μm to 3 mm, the majority of obtained surfaces in the visual sense is typically ladder-shaped rough by the direct stack from the collection of cross-sections (slices) under the low resolution or even image noise contained during the signal or image processing. Furthermore, for the higher resolution, the processing of image and signal is also low efficiency, and data storage capacity is over the level of gigabyte (GB). To overcome the above situations, the purpose of this work in the computational approach is to propose a new framework for getting a fast and smooth super-resolution 3D reconstruction from limited low-resolution sampling (collected data). Here, the framework integrating with the traditional approach of computed tomography from the signal processing to inverse Radon transform (IRT) and the core mathematical approach by the variational formulation is elucidated as follows. What is more, due to the results under the super-resolution, the quantifiable approach is unveiled under the viewpoint of discrete geometry by computing the standard deviation of mean curvatures for the triangular meshes of final surfaces to indicate the stable level of the global smoothness.

II. Procedures with Experimental Demonstrations

For the fast signal processing of the raw dataset collected by the ASynchronous OPtical Sampling (ASOPS) THz-TDS system (Menlo TERA ASOPS, Menlo Systems) [2], the first step (called Time-MAX) is to acquire the maximum peak of time-resolved signal with respect to the time sampling. Here the

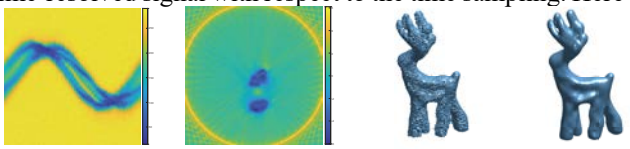

Fig. 1. Illustrations of the fast-reconstructed framework: (a) Representative sinogram by Time-MAX; (b) Cross section (slice) by IRT; (c) Rough reconstruction by input total 218 slices; (d) Smooth result of (c) by the Willmore-based formulation.

Fig. 2. Illustrations of (a) input 109 slices with 1 gap; (b) output from (a); (c) input 55 slices with 3 gaps; (d) output from (c); (e) input 37 slices with 5 gaps; (f) output from (e).

deer model is exemplified with the size 61×300×1000×300 where 61 is the total number of angles from one revolution, 300 is the horizontal spatial sampling, 1000 is the time sampling, and 300 is the vertical spatial sampling which is the corresponding cross-section (slice). And then, as Fig. 1(a) depicted, the representative sinogram can be obtained from the dataset (300×300×61) after the signal processing [3]. Following that, by inverse Radon transform (IRT), the slices can be procured as Fig. 1(b) demonstrated where the resolution and the number of the slice are set as 288 and 218 respectively for removing extra unnecessary portions of scanning to reduce the further processing time. For the better effect of reconstructed slices, the type of interpolation has opted as the cubic convolution. The filter is used by multiplying the Ram-Lak filter by a Hann window [4]. By now, the rough object can be constructed by the specified segmented threshold as most works did, and Fig. 1(c) is portrayed by stacking a total of 218 informative slices under the low resolution with N = 288. Remark that all implementations are coded with the computer programming language: MATLAB_R2022a® in the operating system: macOS Monterey (Version 12.3) equipped with the 2.3 GHz 8-Core Intel Core i9 processer and the 16 GB 2667 MHz DDR4 memory.

To smooth the surface, the variational model is considered as the Willmore-based formulation

$$u_\varepsilon^* = \arg\min_{u_\varepsilon^{in} \le u \le u_\varepsilon^{ex}} \frac{1}{2\varepsilon}\int_{\Re^D}\left(\varepsilon\Delta u - \frac{1}{\varepsilon}W'(u)\right)^2 dx$$

where the rough object $u \in \Re^D$ (in this case D stands for three dimensions where this model works for $D = 2$ in the Euclidean space $\Re^D$) with the linear obstacle restriction $u_\varepsilon^{in} \le u \le u_\varepsilon^{ex}$ formed by the interior restriction u_ε^{in} and exterior restriction u_ε^{ex} is under the formulation with respect to the double-well potential $W(u) = \frac{1}{2}u^2(1-u)^2$ with its first order derivative $W'(u) = u(u-1)(2u-1)$, and the parameter ε as the diffuse interface width, with Γ-convergence and phase-field approximation to the Willmore-based functional energy

$$W_\varepsilon(u) = \frac{1}{2\varepsilon}\int_{\Re^D}\left(\varepsilon\Delta u - \frac{1}{\varepsilon}W'(u)\right)^2 dx \xleftarrow{\Gamma(L^1(\Omega))}{\varepsilon\to 0} W(\Omega) = \frac{1}{2}\int_{\partial\Omega}|\kappa|^2 dH^{D-1}$$

with the mean curvatures κ on the boundary $\partial\Omega$ and the Hausdorff measure H^{D-1} in $\Re^D$. To approximate the numerical local minimum of above Willmore-based formulation, the algorithm called the projected gradient descent method using the Euler semi-implicit discretization scheme within fast Fourier transform from the corresponding Euler-Lagrange partial differential equation

$$\Delta\left(\varepsilon\Delta u - \frac{1}{\varepsilon}W'(u)\right) - \frac{1}{\varepsilon^2}W''(u)\left(\varepsilon\Delta u - \frac{1}{\varepsilon}W'(u)\right) = 0$$

is constituted in Alg. 1 [5][6]. After iterating step 2 and step 3 of Alg. 1, Fig. 1(d) unveils the final smooth result by the Willmore-based formulation from total 218 slices. What is more, returning to the initial expectation, if only acquiring few slices with gaps (limited sampling), this framework is still available to reconstruct the smooth results as Fig. 2(a)-(f) shown. For the input 37 slices with 5 gaps, the data acquisition time can be at least saved 83% approximately.

Alg. 1. Projected Gradient Descent Method

1: Initialize the input u by the phase-field function and to content with the interior and exterior restriction

$$u_\varepsilon^{in} \le u \le u_\varepsilon^{ex}.$$

2: Implement the restrictions to procure the orthogonal projection

$$u^{d+\frac{1}{2}} = \max(\min(u, u^{ex}), u^{in}).$$

3: Compute the solution u^{d+1} by the numerical Euler semi-implicit discretization applying the fast Fourier transform scheme with the synthetic time step τ_t

$$u^{d+1} = (I_D + \varepsilon\tau_t\Delta^2)^{-1}\left(u^d + \frac{\tau_L}{\varepsilon}\Delta W'(u^{d+\frac{1}{2}}) - \frac{\tau_L}{\varepsilon}W''(u^{d+\frac{1}{2}})\Delta u^{d+\frac{1}{2}} + \frac{\tau_L}{\varepsilon^3}W'(u^{d+\frac{1}{2}})W''(u^{d+\frac{1}{2}})\right).$$

III. Quantifiable Comparisons

After presenting the reconstructed results by few input slices in Fig. 2, the specified gaps are assigned as 1, 3 and 5 so that the collected slices from smaller gaps can be covered by most of slices from larger gaps. To compare the results under the super resolution from at least same limited dataset of low-resolution inputs, the quantifiable approach is proposed by computing the standard deviation (STD) of mean curvatures (MC) σ_{MC} to each vertex of triangular meshes for final surfaces [7][8]. As Tab. 1 reified, the results in the similar level around 20 to 40 herald the effectiveness of reconstructions by less input slices, and also indicate the better smoothness for the lower value since more details will be lost from less input slices with more gaps.

Tab. 1. Comparison of the standard deviation of mean curvatures for the smooth results with different input slices and gap(s).

Input slices	218	109	55	37
Gap(s)	0	1	3	5
σ_{MC}	44.7612	30.3103	20.1637	16.3767

IV. Summary with Future Concentration

The reconstructed framework for fast, smooth THz 3D super-resolution surface reconstruction under the costing time level of minutes from storing in the low-resolution limited data is instantiated in this paper by integrating with the traditional approach of computed tomography and the Willmore-based formulation. Moreover, the quantifiable approach by computing the standard deviation of mean curvatures is constituted to indicate the effectiveness of how many slices are input to improve the efficiency for fast, smooth reconstruction.

For future concentration, some are in progress. To modify the framework blended with imaging denoising, imaging segmentation, and imaging registration to improve the further quality in THz imaging and other imaging fields (e.g. X-ray radiation, magnetic resonance imaging, and ultrasound imaging) is one of the realizable extensions. Especially for the properties of THz waves, the information of frequency domain associated with spectral fingerprints can be applied as signal processing to identify or even reconstruct different matters in the field of security sensing or sample analysis. Last but not least, together with the variational modelling, the crucial perspectives could be by adapting the appropriate functional energy with its corresponding partial differential equation and developing the rapid and high accurate numerical algorithm for solving the variational problems and other inverse imaging conundrums.

References

[1] H. Guerboukha, K. Nallappan, and M. Skorobogatiy, "Toward real-time terahertz imaging," *Adv. Opt. Photon*, 10, 843–938, 2018.

[2] A. Stoica, Y.-M. Sheu, D. A. Reis, and R. Clarke, "Wideband detection of transient solid-state dynamics using ultrafast fiber lasers and asynchronous optical sampling," *Opt. Express*, 16, 2322–2335, 2008.

[3] Y. -C. Hung and S. -H. Yang, "Terahertz Deep Learning Computed Tomography," *2019 44th International Conference on Infrared, Millimeter, and Terahertz Waves (IRMMW-THz)*, 1–2, 2019.

[4] A. C. Kak and Malcolm Slaney, "Principles of computerized tomographic imaging," *Society of Industrial and Applied Mathematics*, 49–112, 2001.

[5] E. Bretin, F. Dayrens, and S. Masnou, "Volume reconstruction from slices," *SIAM Journal on Imaging Sciences*, 10(4), 2326–2358, 2017.

[6] K. Chen, "Introduction to variational image-processing models and applications," *International Journal of Computer Mathematics*, 90, 1–8, 2013.

[7] M. Meyer, M. Desbrun, P. Schröder, and A.H. Barr, "Discrete Differential-Geometry Operators for Triangulated 2-Manifolds," *Visualization and Mathematics III*, 35-57, 2003.

[8] J. Wang and Z. Yu, "A Novel Method for Surface Mesh Smoothing: Applications in Biomedical Modeling," *Proceedings of the 18th International Meshing Roundtable*, 195–210, 2009.